Heliyon 10 (2024) e34660

Contents lists available at ScienceDirect

Heliyon

journal homepage: www.cell.com/heliyon

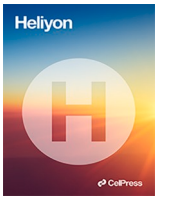

Research article

The circular RNA circ_0001742 regulates colorectal carcinoma proliferation and migration via the MicroRNA-431-5p/ALG8 axis

Jiahao Huang [a,b,c,e,1], Fengyun Cong [a,c,1], Yang Zhao [d], Jinglian Chen [a,c], Tao Luo [a,c,**], Weizhong Tang [a,c,*]

[a] Department of Gastrointestinal Surgery, Affifiliated Tumor Hospital, Guangxi Medical University, Nanning, China
[b] Department of Colorectal and Anal Surgery, The First Affifiliated Hospital, Guangxi Medical University, Nanning, China
[c] Guangxi Clinical Research Center for Colorectal Cancer, Nanning, China
[d] Department of Radiology, Affiliated Tumor Hospital, Guangxi Medical University, Nanning, China
[e] Guangxi Key Laboratory of Enhanced Recovery after Surgery for Gastrointestinal Cancer, Guangxi, China

ARTICLE INFO

Keywords:
Circ_0001742
MiR-431-5p
ALG8
Colorectal cancer
Migration

ABSTRACT

Background: Accumulating studies have found that circular RNAs (circRNAs) have a regulatory effect in a variety of tumors. However, to date, the relationship between specific circRNAs and colorectal cancer (CRC) remains elusive.
Methods: An RNA-sequencing method based on different metastatic potential of CRC cell lines was applied to evaluate the circRNA expression profile. Additionally, we conducted a series of experiments to assess the relationship between circRNAs and CRC progression.
Results: Circ_0001742 was upregulated in CRC cells with high metastatic potential, and circ_0001742 overexpression was observed to facilitate proliferation, migration and metastasis while knockdown will inhibit. More importantly, we found that circ_0001742 acted as a sponge for miR-431-5p, thus affecting ALG8 levels and the development of CRC.
Conclusions: This study demonstrated an essential function for the circ_0001742/miR-431-5p/ALG8 axis in CRC development, and it may be a promising therapeutic target for CRC.

1. Introduction

The incidence and mortality of colorectal cancer (CRC) worldwide are in third and second place, respectively [1]. Normally, CRC lacks obvious symptoms until it reaches an advanced stage. At present, the high level of disease recurrence in CRC patients has not decreased with the improvement of therapeutics, and the 10-year survival rate of patients is approximately 20 % [2,3]. Therefore, these findings suggest that it is imperative to explore the specific mechanisms of disease progression in CRC patients [4].

There is increasing evidence that different types of cancer are influenced by non-coding RNAs (ncRNAs) such as microRNAs (miRNAs), long noncoding RNAs (lncRNAs), and circular RNAs (circRNAs) [5,6]. Unlike traditional linear RNAs, circular RNAs

* Corresponding author. Department of Gastrointestinal Surgery, Affiliated Tumor Hospital of Guangxi Medical University, 71 Hedi Road, Nanning, Guangxi Zhuang Autonomous Region, China, 530021.
** Corresponding author. Department of Gastrointestinal Surgery, Affiliated Tumor Hospital of Guangxi Medical University, 71 Hedi Road, Nanning, Guangxi Zhuang Autonomous Region, China, 530021.
E-mail addresses: luotao@gxmu.edu.cn (T. Luo), tangweizhong@gxmu.edu.cn (W. Tang).
[1] These authors have contributed equally to this work.

https://doi.org/10.1016/j.heliyon.2024.e34660
Received 26 December 2023; Received in revised form 11 July 2024; Accepted 15 July 2024
Available online 15 July 2024

Abbreviations

circRNAs	Circular RNAs
CRC	Colorectal cancer
miRNAs	MicroRNAs
mRNAs	Messenger RNAs
ALG8	Alpha-1,3-glucosyltransferase
qRT−PCR	Quantitative real-time polymerase chain reaction
TPM	Transcripts per million
AGO2	Anti-Argonaute2
EP	Eppendorf
ELC	Enhanced chemiluminescence
IHC	Immunohistochemistry
WT	Wild-type
ER	Oestrogen receptor
RBPs	RNA-binding
OE	Proteins over expression

(circRNAs) are a special class of noncoding RNAs without 5′ caps and 3′ polar or polyadenylation tails [7,8]. Therefore, circRNAs are not affected by RNA exonuclease and hence exhibit pivotal regulatory functions. With the development of next-generation sequencing, circRNAs have been proven to be tissue development-specific and involved in cancer growth and metastasis [9,10].

MicroRNAs (miRNAs) are small noncoding RNAs that typically inhibit the translation and stability of messenger RNAs (mRNAs), controlling genes involved in cellular processes such as inflammation, cell-cycle regulation, stress response, differentiation, apoptosis, and migration [11]. Emerging evidence in recent years has shown circRNAs that affect the development of tumour cells by sponging certain miRNAs to regulate the whole transcript profile [12]. It is well known that miR-7 has a tumour inhibitory effect, but overexpression of circRNA ciRS7 can antagonize this effect [13]. Different types of cancer cells have different expression disorders of circRNAs; that is, circRNAs can either inhibit or promote tumour cell growth [14,15]. However, no matter what role circRNAs play in promoting or inhibiting tumour cell growth, it is certain that they do come into play, so it is meaningful to study their specific mechanism for cancer treatment. Nevertheless, the expression pattern, biological function and underlying mechanism of certain circRNAs in CRC progression and metastasis have not been fully revealed.

Based on this, we are eager to find the relevant circRNAs that affect colorectal cancer cells. When sequencing different CRC cell subsets, we found that hsa_circ_0001742 is closely involved in the activity of CRC cells. Additionally, we demonstrated that circ_0001742 was greatly upregulated in CRC tissues. In addition, we also found that circ_0001742 promoted the invasion and metastasis of CRC. Interestingly, we also found that miR-431-5p and alpha-1,3-glucosyltransferase (ALG8) may be related to circ_0001742. MiR-431-5p is dysregulated in various cancers and plays an important function in the development of cancer [16]. Researchers have found miR-431-5p to be down-regulated in colorectal cancer cells and tissues, and miR-431 to be down-regulated as well [17]. ALG8 is a Enzyme for protein N-glycosylation, it encodes a member of the ALG6/ALG8 glucosyltransferase family. The encoded protein catalyzes the addition of the second glucose residue to the lipid-linked oligosaccharide precursor for N-linked glycosylation of proteins [18,19]. ALG8 is upregulated in colon cancer tissues compared to normal tissues. Overexpression of the ALG8 gene predicts poor overall survival and disease-free survival in colon cancer patients [20]. Circ_0001742 might function as a sponge of miR-431-5p, thereby synergistically increasing the level of ALG8. Most importantly, our results highlighted the underlying mechanism of tumorigenicity in CRC and suggested that circ_0001742 is a valuable therapeutic target(Fig. 1A).

2. Material and methods

2.1. Tissue specimens and cell lines

Twenty-nine samples of CRC and corresponding normal tissues were obtained from patients (no neoadjuvant chemotherapy or chemoradiotherapy before surgery) who underwent surgery at the Department of Gastrointestinal Surgery, the Affiliated Tumor Hospital of Guangxi Medical University, from June to December 2019. All tissue specimens were immediately stored at −80 °C after surgical excision. This study was approved by the ethics committee.

The CRC cancer cell lines LoVo, HCT116, SW480, and DLD1 were all derived from the Cell Bank of the Chinese Academy of Sciences (Shanghai, China) and cultured in DMEM (Gibco, NY, USA) supplemented with 10 % FBS (Gibco, NY, USA). Culture conditions: 37 °C, 5 % CO2 and 95 % air.

2.2. RNA sequencing and analysis of human circRNAs

Total RNA in the LoVo, HCT116, SW480, and DLD1 cell lines was extracted using the RNeasy Plus Mini Kit (Qiagen, CA, U.S.A.). 1 RiboMinus Eukaryote Kit (Qiagen, Valencia, CA) was used to process RNA. A CDNA library was constructed after the linear RNA was

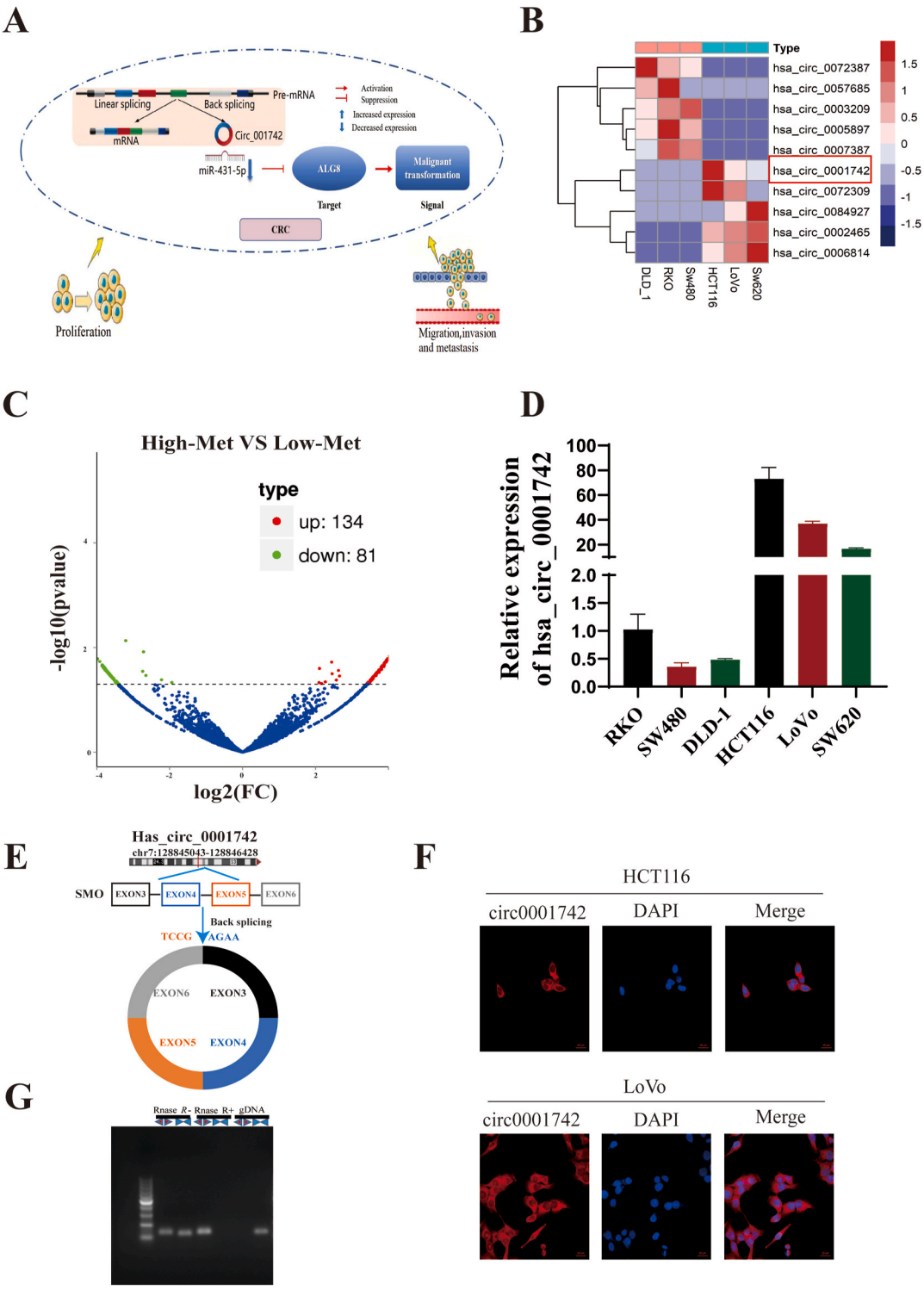

Fig. 1. Identification and expression of hsa_circ_0001742 in CRC tissues and cells. (A) Mechanism diagram of this work. (B) The heatmap showed the top 10 circRNAs differentially expressed in the highly invasive cell group compared to the low invasive cell group. The red boxes marked the circular RNAs that we were interested in.(C) The volcano plot showed that 215 circRNAs were differentially expressed in the highly invasive cell group compared with the low invasive cell group. (D) Expression of hsa_circ_0001742 in different colorectal cancer cell lines, based on real-time quantitative PCR method. (E) The diagram showed the connection structure and partial sequence of Hsa_circ_0001742. (F) Hsa_circ_0001742 was detected by FISH in HCT116 and LoVo. Nuclei were stained with 4′,6′-diamidino-2-phenylindole. Scale bar = 20 μm. (G) Total RNA from cells with or without RNase R treatment was subjected to PCR.

removed [21]. The constructed cDNA library was sequenced on an Illumina NovaSeq 6000 (Illumina, San Diego, CA), and the sequenced results were counted. First, all RNA sequencing reads were located in the human reference genome (GRCh37/hg19), and then unmapped reads were used to identify circRNAs of find_circ [22]and CIRI2 [23]. TPM (Transcripts per million) was used to normalize the original data, and edgeR was used to perform scaling to normalize and adjust the factors before difference analysis [24]. DEGseq (2010) of the R software package was used for difference analysis.

2.3. Quantitative real-time polymerase chain reaction (qRT–PCR)

Total RNA was isolated from CRC cell lines using TRIzol reagent (Invitrogen, Carlsbad, CA, USA). Total RNA (1 μg) was incubated for 30 min at 37 °C with 3 U/μg RNase R (Epicentre Technologies) to verify the existence of circRNA [25]. In the analysis of circRNA, mRNA and miRNA, Prime Script RT Master Mix was used for the first two (Takara, Dalian, China) to synthesize cDNA, while RevertAid first strand cDNA was used for the latter to synthesize reverse transcription-specific cDNA (Thermo Scientific, Mountain View, CA, USA). qRT–PCR was performed with a QuantiTect SYBR Green PCR kit (Qiagen, CA, USA), and the relative fold-change was calculated by the 2-△△Ct method. GAPDH was used as an internal control for circRNA and mRNA detection, and U6 was used for miRNA evaluation (the relevant primers for qRT–PCR are listed in Supplementary Table S1).

2.4. Fluorescence in situ hybridization (FISH)

The circRNA probe and kit used in this fluorescence in situ hybridization are from RiboBio (Guangzhou, China). The specific detection steps were as follows: HCT116 and LOVO cells were soaked in formalin (4 %, 15 min). After prehybridization with PBS, the cells were put into the hybridization solution for formal hybridization (37 °C, 30 min). DAPI (4',6-diamino-2-phenylindol) (Beyotime, China) was used for staining, and then a Zeiss LSM880 confocal microscope system (Leica Microsystem, Mannheim, Germany) was used to obtain images.

2.5. Cell transfection

The cells were inoculated into a 6-well plate, and transient transfection was performed when the cell development reached 50–60 %. Si-RNAs targeting circRNA, miRNA mimics and inhibitors were designed and synthesized by Hanying (Shanghai, China). Lipofectamine 2000 (Invitrogen) was used for transfection. PcDNA_cirRNA or empty vector (Shanghai Hanying, China) was transfected into HEK-293T cells to obtain overexpressed circRNA. The whole coding region of the gene was cloned into pcDNA3.1 (Hanying, Shanghai, China) to obtain the overexpressed target gene. The negative control group was lentivirus-free (sequences are listed in Supplemental Table S1).

2.6. RNA immunoprecipitation assay

RNA immunoprecipitation (RIP) detection: lysate containing human *anti*-Argonaute2 (AGO2) or negative control mouse IgG was prepared, and cells were placed in the above lysate. The lysed cell sample was incubated with protease K and then analyzed with TRIzol reagent to obtain RNA. The RNA obtained in the above steps was analyzed by RT–PCR.

2.7. Luciferase reporter assay

HEK293T cells were seeded in 96-well plates and transfected with circ_0001742 or miR-431-5p wild-type or mutant fragment 3′UTR plasmids using liposome 3000 (Invitrogen, CA). Luciferase activity was measured 48 h after transfection.

2.8. Cell proliferation assay

The proliferation of Colorectal cancer cells was measured using Cell-Counting Kit 8 (CCK8; Dojindo Molecular Technologies). Transfected cells (3×10^3 cells/well) were seeded in 96-well plates. An incubation period of 24, 48, 72, 96, and 120 h was followed by the addition of 20 mL of CCK-8 solution in each well. A Multiskan Go spectrophotometer (Thermo Fisher Scientific, Inc.) was used to measure the absorbance at 450 nm. Each CCK-8 test group was replicated three times.

2.9. Transwell and invasion assay

Cells were placed in 24-well plates for the Transwell assay: Cells and 10 % foetal bovine serum were incubated in the upper and lower chambers of the Transwell, respectively. After 24 h, the cells that infiltrated below the membrane were fixed with paraformaldehyde (4 %) and stained with haematoxylin. After 10 min, the haematoxylin was removed, the stem cells were gently pipetted, and the cells were counted.

2.10. Cell cycle and apoptosis assay

After 48 h of transfection, the cells in each group were rinsed with precooled PBS and resuspended in PBS binding buffer. Annexin

V-FITC (10 μL) was added to the resuspended cell solution, gently shaken until the dye solution was thoroughly mixed with the cell suspension, and incubated for 20 min away from light. Five microlitres of PI was added 10 min before apoptosis detection to detect apoptosis by flow cytometry.

2.11. Wound healing assay

The cells were grown in DMEM containing 10 % FBS. After 24 h of cell generation, the cells were inoculated into 24-well plates, and the degree of fusion of the monolayer reached 70–80 %. Without changing the medium, a 1 mL spear head was used to lightly scratch the monolayer between cells (the spear head was perpendicular to the plate hole). A scratch was made perpendicular to the first scratch in the same way. After the scratch, the plate was gently washed with medium twice to remove the shed cells. Fresh medium was added to each well. After 48 h of cell growth, the cells were washed twice with PBS and then fixed (30 min) with paraformaldehyde (3.7 %). Cells were stained with crystal violet (1 %), photographed and counted with an inverted microscope [26].

2.12. Western blotting

The level of protein expression by Western blotting [27]. Cut the tissue to be studied in the ice. The tissue is transferred to a EP tube and immersed in liquid nitrogen for rapid freezing. One millilitre of RIPA lysate was added into the EP tube and centrifuged after full blowing (3000×*g*, 10 min). The supernatant obtained by centrifugation was transferred to a new EP tube, and protein expression was detected with a protein kit. Another part of the supernatant was boiled (100 °C) for 5 min, and the protein was denatured followed by electrophoresis, with 20 μg protein per lane. After electrophoresis, the separated proteins were transferred and washed, and then ELC (Enhanced chemiluminescence) chemiluminescence reagent was added (with attention given to the development of light). A gel imaging system was used to expose the bands and take pictures, and a gel image processing system was used to analyse the grey value of the target protein.

2.13. Xenograft tumour model

After the approval of the Ethics Committee, 4-week-old BALB/c nude mice (Chinese Academy of Sciences, Shanghai, China) were divided into 8 mice per group. LoVo cells were inoculated separately for LoVo cells with circ_0001742 knockdown and LoVo cells with circ_0001742 knockdown and ALG8 overexpression. The mice were killed 8 weeks after inoculation. The tumour was removed for diameter measurement and staining.

2.14. Immunohistochemistry

Immunohistochemistry (IHC) was performed on FFPE tissue sections [28]. The primary antibody used was *anti*-ALG8 (1:100, #PA5-50317, Thermo Scientific). The tissue sections were incubated with the primary antibody followed by the secondary antibody. The incubation conditions of the primary antibody were 4 °C for 12 h. The incubation conditions of the secondary antibody were 37 °C for 1 h. After incubation, the sections were dehydrated. The results of the experiment were first evaluated by two staff members and then summarized. The composite score was based on both the proportion of positively stained tumour cells and the intensity of staining. Finally, a total score <6 was considered negative, and a total score ≥ 6 was considered positive.

2.15. Bioinformatics analysis

The sequence of target circRNA was obtained from circbase (http://www.circbase.org). TargetScan (http://www.targetscan.org/) and miRanda (http://www.microrna.org/) were used to predict the binding sites between circRNAs and miRNAs. GO analysis was conducted to construct meaningful annotations of genes and gene products in a wide variety of organisms through the DAVID database (http://david.abcc. ncifcrf.gov).

2.16. Statistical analysis

SPSS19.0 (IBM, SPSS, Chicago, IL, USA) was used for data analysis in this study. Data are expressed as the mean ± SD. $P < 0.05$ indicated significance. Intergroup comparisons, intragroup comparisons and correlation analyses were performed using Student's *t*-test, one-way ANOVA, and Pearson's correlation coefficients, respectively.

3. Results

3.1. The expression of circ_0001742 in CRC cells

mRNA and circRNA expression in CRC cell subgroups with different metastatic potential was analyzed by RNA sequencing (Fig. 1B). The invasive ability of these subgroups was proven as previously described [29]. High metastatic potential cells consisted of HCT116, LoVo and SW620 cells, and low metastatic potential cells consisted of RKO, DLD-1 and SW480 cells. When identifying the circRNAs involved in the deregulation of the initial step of transfer (Fig. 1B), we found that 215 circRNAs were differentially expressed

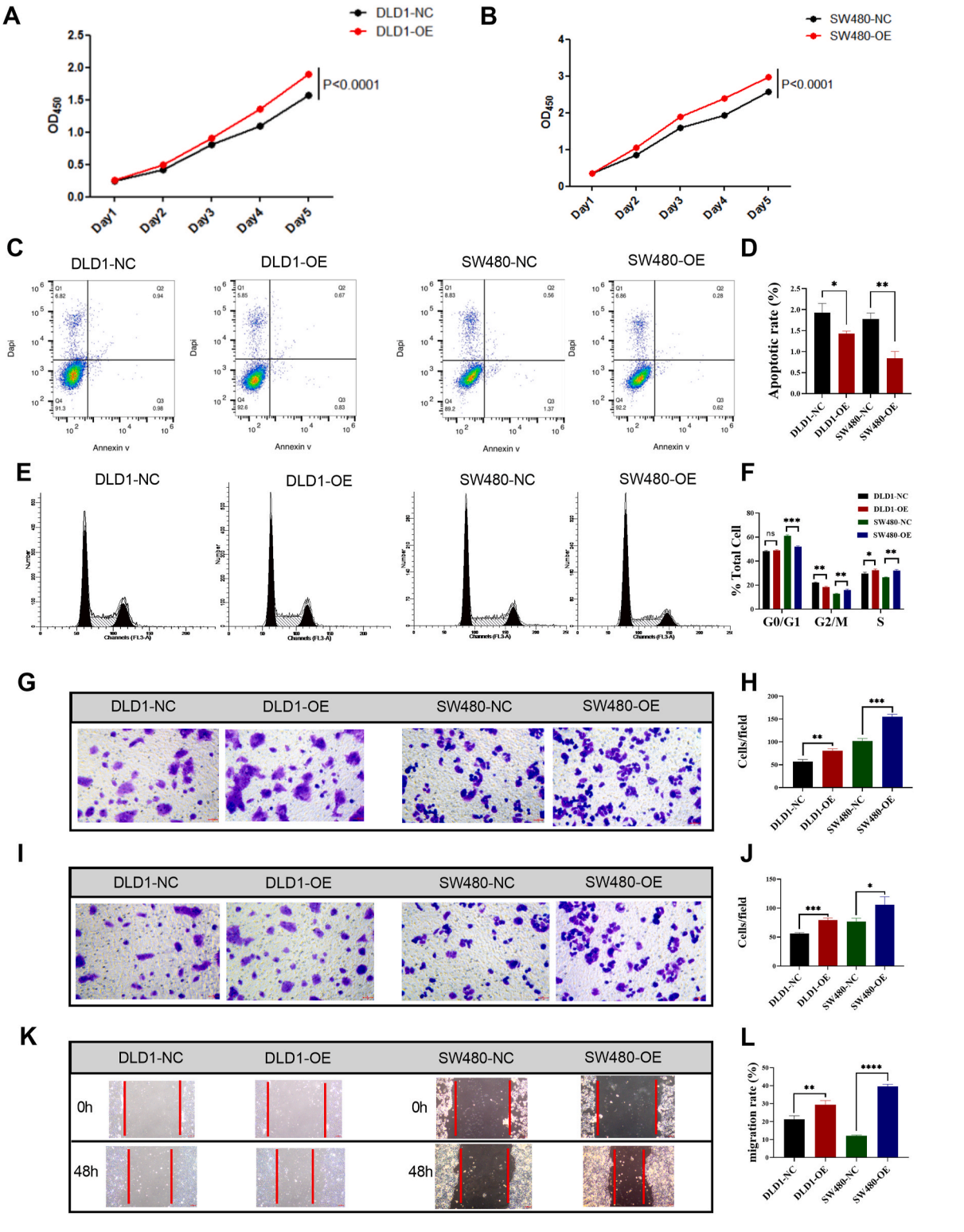

(caption on next page)

Fig. 2. Hsa_circ_0001742-overexpression (OE) promote CRC cells proliferation, apoptosis, cell cycle, invasion and migration. (A, B) CCK-8 assays were performed using DLD1 and SW480 with or without hsa_circ_0001742-OE. (C, D) The results of flow-through apoptosis experiments showed that compared with the control cells, the apoptosis of CRC cells in the circ_0001742-OE group was significantly reduced. (E, F) The results of flow cytometry cycle experiments showed that compared with the control cells, in the circ_0001742-OE group, the number of cells in the G0 phase was significantly decreased, and the number of cells in the G2 and S phases was significantly increased in SW480 cells. The overexpression of circ_0001742 had no significant effect on the G0 phase of DLD1 cells, the cells in the G2 phase were significantly reduced, and the cells in the S phase were significantly increased. (G, H) The results of Transwell experiments showed that compared with the control cells, the migration ability of CRC cells in the circ_0001742-OE group was significantly increased. (I, J) The results of Matrigel-Transwell experiments showed that compared with the control cells, the invasive ability of CRC cells in the circ_0001742-OE group was significantly increased. (K, L) The results of the Scratch test showed that compared with the control cells, the migration ability of CRC cells in the circ_0001742-OE group was significantly increased. *P < 0.05, **P < 0.01, ***P < 0.001.

between different metastatic potential cells. Among these, 134 were greatly upregulated, while 81 were downregulated (|log2 (fold change)| > 1; Q-value <0.05; read count >40 (Fig. 1C). Additionally, circ_0001742 was found to be greatly upregulated in CRC cell subsets with high metastatic potential by real-time quantitative polymerase chain reaction (RT−qPCR) (Fig. 1D).

3.2. Characterization of circ_0001742 in CRC

According to circBase [30], circ_0001742 has a total length of 727 Nt and consists of the SMO gene (q34.3:135,810,490–135,907, 228). We confirmed the circ_0001742 connection (Fig. 1E) and the predominant cytoplasmic distribution of circ_0001742 in HCT116 and LoVo cells (Fig. 1F). The PCR results showed that the circular transcript of circ_0001742 could only be amplified by divergent primers in cDNA. RNase R treatment indicated that circ_0001742 was much more stable than linear mRNA (Fig. 1G).

3.3. Effects of circ_0001742 overexpression on CRC cells in vitro

To investigate the functions of circ_0001742 in CRC cells in vitro, we constructed circ_0001742 overexpression stable cell lines by transfection of circ_0001742-specific vector full-length cDNA. As shown in Fig. 2A–B, the overexpression of circ_0001742 in DLD-1 and SW480 cells boosted their proliferation. We also found that silencing circ_0001742 promoted tumour cell apoptosis, while overexpressing circ_0001742 decreased cancer cell apoptosis (Fig. 2C–D). Furthermore, knockdown of circ_0001742 induced G0 phase cell cycle arrest in LoVo and HCT116 cells. Overexpression of circ_0001742 decreased the proportion of cells in G0/G1 phase and increased the proportion of cells in S phase, while the proportion of cells in G2/M phase increased in SW480 cells. Conversely, a similar trend was not observed in DLD-1 cells (Fig. 2E–F). Subsequently, we also found that overexpression of circ_0001742 greatly enhanced the migration and invasion activity of both DLD-1 and SW480 cells (Fig. 2G-L).

We then suppressed the level of circ_0001742 in LoVo and HCT116 cells using lentiviral delivery and successfully constructed circ_0001742 knockdown stable cell lines that specifically targeted the back-spliced junction site of circ_0001742 and reduced the level of circ_0001742 (sFig. 1A–C). Knockdown of circ_0001742 remarkably impaired the proliferation of LoVo and HCT116 cells (Fig. 3A–B). The results indicated that silencing circ_0001742 promoted tumour cell apoptosis (Fig. 3C–D). Furthermore, we found that circ_0001742-KD could induce G0 phase cell cycle arrest in LoVo and HCT116 cells (Fig. 3E–F). On the other hand, the enhancement in migration capacity was greatly reversed when circ_0001742 was inhibited (Fig. 3G-L). Collectively, these results revealed that circ_0001742 had a positive effect on the progression of CRC cells.

3.4. Circ_0001742 serves as a sponge for miR-431-5p, and miR-431-5p directly targets the ALG8 3′-UTR

Given that the preliminary results indicate that circ_0001742 mainly exists in the cytoplasm, we assumed that circ_0001742 acted as a miRNA sponge and sequestered miRNAs to inhibit gene regulation. We used starBase (website: http://starbase.sysu.edu.cn/index.php) to predict that circ_0001742 could bind to miR-431-5p. The bioinformatics algorithms PicTar (website: https://pictar.mdc-berlin.de/) and TargetScan (website: http://www.targetscan.org) predicted that ALG8 was the target gene of miR-431-5p (Fig. 4A). We observed that after cotransfection of circ_0001742 and miR-431-5p-wild-type (WT) genes, luciferase activity in cells was greatly reduced. A sustained decrease in luciferase activity was observed after cotransfection of miR-431-5p and ALG8–3′UTR-WT in HEK293 cells (Fig. 4B). Notably, the luciferase activity was greatly improved after transfection with overexpressed circ_0001742 and miR-431-5p in the ALG8-3′ UTR WT cell line. Collectively, these results illustrate that miR-431-5p could target the ALG8 3′-UTR. RIP analysis showed that compared to the IgG group, more circ_0001742/miR-431-5p/ALG8 was pulled down by the anti-Ago2 antibody in HCT116 and LoVo cells (Fig. 4C). Furthermore, miR-431-5p expression was greatly downregulated in cells overexpressing circ_0001742, while the opposite result was obtained after circ_0001742 knockdown, and the expression of ALG8 was positively correlated with circ_0001742. ALG8 expression was notably increased in cells overexpressing circ_0001742, while the opposite result was obtained in circ_0001742-knockdown cells (Fig. 4D–E). These results indicated that miR-431-5p could directly target the ALG8 3′-UTR, while circ_0001742 could affect the function of CRC cells by serving as a miR-431-5p sponge.

3.5. Circ_0001742 and circ_0001742/miR-431-5p/ALG8 axis

We revealed that treatment with the miR-431-5p inhibitor and overexpression of ALG8 in circ_0001742-knockdown cells promoted

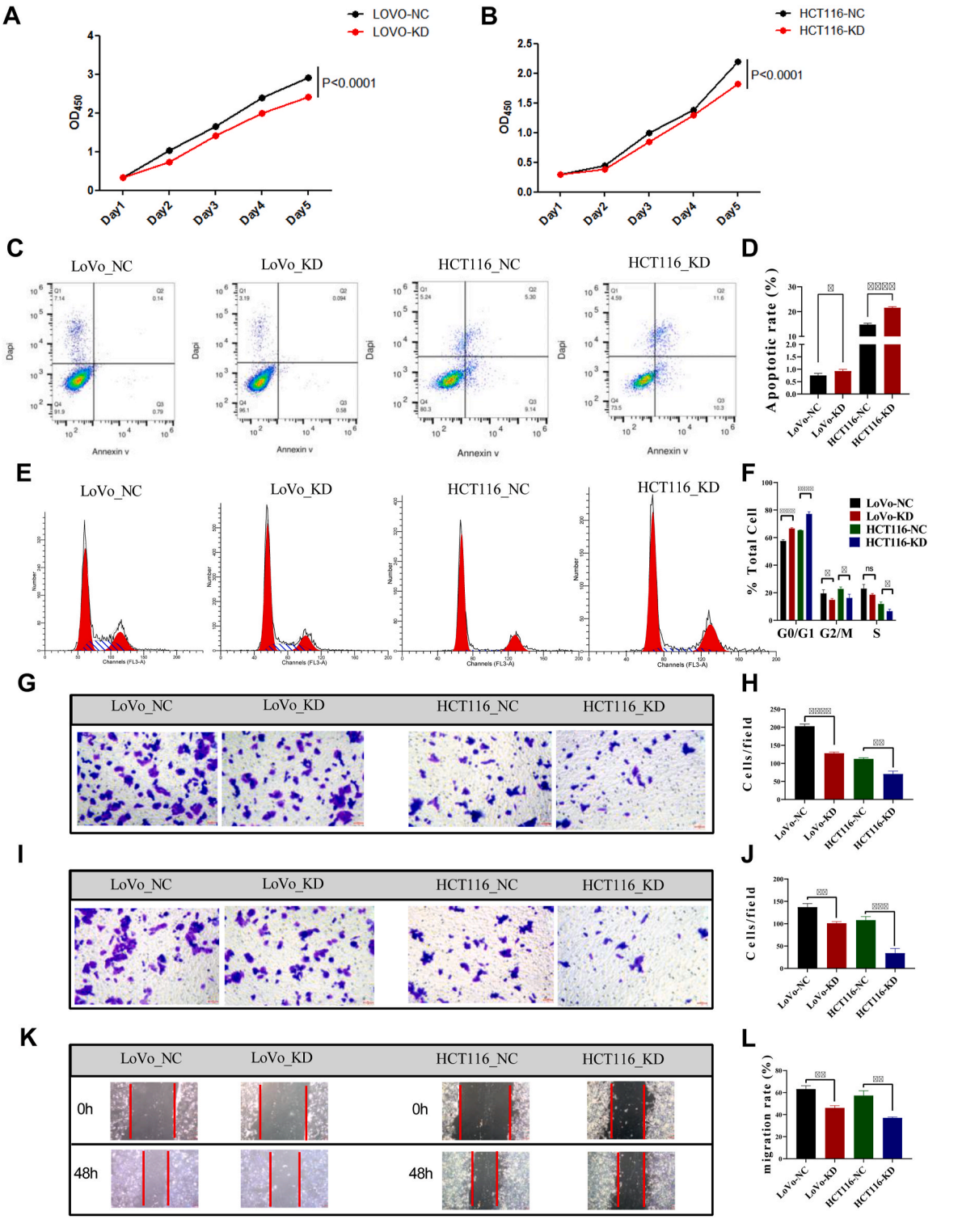

(caption on next page)

Fig. 3. Hsa_circ_0001742-knockdown (KD) suppressed CRC cells proliferation, apoptosis, cell cycle, invasion and migration. (A, B) CCK-8 assays were performed using HCT116 and LoVo with or without hsa_circ_0001742-KD. (C, D) The results of flow-through apoptosis experiments showed that compared with the control cells, the apoptosis of CRC cells in the circ_0001742-KD group was significantly increased. (E, F) The results of flow cytometry cycle experiments showed that compared with the control cells, the number of cells in the G0 phase in the circ_0001742-KD group was significantly increased, and the number of cells in the G2 and S phases was significantly decreased. (G, H) The results of Transwell experiments showed that compared with the control cells, the migration ability of CRC cells in the circ_0001742-KD group was significantly decreased. (I, J) The results of Matrigel-Transwell experiments showed that compared with the control cells, the invasive ability of CRC cells in the circ_0001742-KD group was significantly decreased. (K, L) The results of the Scratch test showed that compared with the control cells, the migration ability of CRC cells in the circ_0001742-KD group was significantly decreased. *P < 0.05, **P < 0.01, ***P < 0.001.

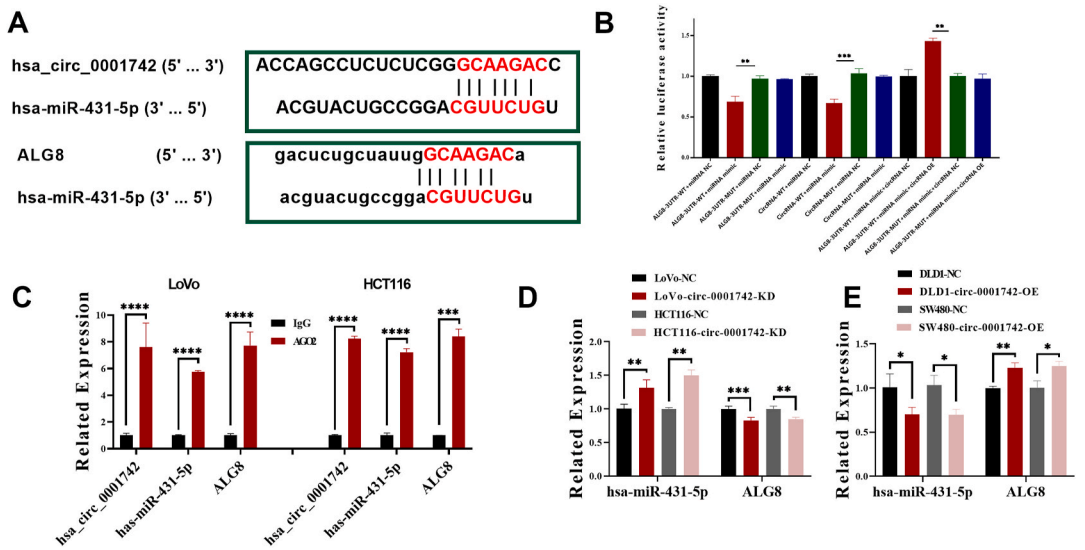

Fig. 4. Mechanism of action of hsa_miR_431-5p with hsa_circ_0001742 and ALG8 ceRNA. (A) A schematic drawing showing the putative hsa_miR_431-5p binding sites with respect to hsa_circ_0001742 and ALG8. (B) Luciferase reporter assays were reported in HEK293T cotransfected with hsa_circ_0001742 and ALG8 reporter plasmid (or the corresponding mutant reporter) and the indicated hsa_miR_431-5p.(C) RIP experiments were performed using an anti-AGO2 antibody and LoVo and HCT116 cells. (D, E) Hsa_miR_431-5p/ALG8 expression after hsa_circ_0001742 knockdown and overexpression. (F) Hsa_circ_0001742/hsa_miR_431-5p/ALG8 expression after hsa_circ_0001742 knockdown and filling ALG8 after knockdown of hsa_circ_0001742. *P < 0.05, **P < 0.01, ***P < 0.001.

their proliferative capacity (Fig. 5A–B). Further investigation revealed that silencing of miR-431-5p and overexpression of ALG8 in circ_0001742-knockdown cells inhibited tumour cell apoptosis (Fig. 5C–D). Furthermore, we found that knockdown of miR-431-5p and overexpression of ALG8 increased the proportion of S phase and G2/M phase cells in circ_0001742-knockdown cells (Fig. 5E–F).

Knockdown of miR-431-5p and overexpression of ALG8 remarkably restored the cell migration and invasion ability in circ_0001742-knockdown cells (Fig. 6A–B). As expected, knockdown of miR-431-5p and overexpression of ALG8 greatly boosted the migration ability of both circ_0001742-knockdown LoVo and HCT116 cells in the transwell migration and invasion(Fig. 6C–D). Silencing of circ_0001742 greatly reduced the expression of ALG8 in CRC cells. These results confirmed that circ_0001742 could promote CRC progression via the miR-431-5p/ALG8 axis (Fig. 6E–F,sFig2). In conclusion, circ_0001742 promotes the progression of CRC cells.

3.6. Circ_0001742 correlated with prognosis

Next, we explored the expression of circ_0001742, miR-431-5p and ALG8 in 29 groups of matched sets of CRC tissues and corresponding normal colorectal tissues. Tissue data demonstrated that circ_0001742 and ALG8 were greatly increased in CRC tissues compared with corresponding normal tissues, while miR-431-5p was not greatly increased in CRC tissues (Fig. 7A–C). In addition, correlation analysis demonstrated that circ_0001742 expression was positively correlated with ALG8 expression (R = 0.169, Fig. 7D). Furthermore, Kaplan–Meier analysis revealed that CRC patients with decreased expression of circ_0001742 had a tendency towards longer overall survival than patients with high circ_0001742 expression(Fig. 7E), and the results of multivariate analysis showed that the expression of circ_0001742 correlated with the prognosis of patients(P = 0.048,Table S2). Low expression of circ_0001742 was positively correlated with clinical stage, although the P value was greater than 0.05(Table S3). Therefore, we concluded that high circ_0001742 expression is correlated with poor prognosis in CRC patients.

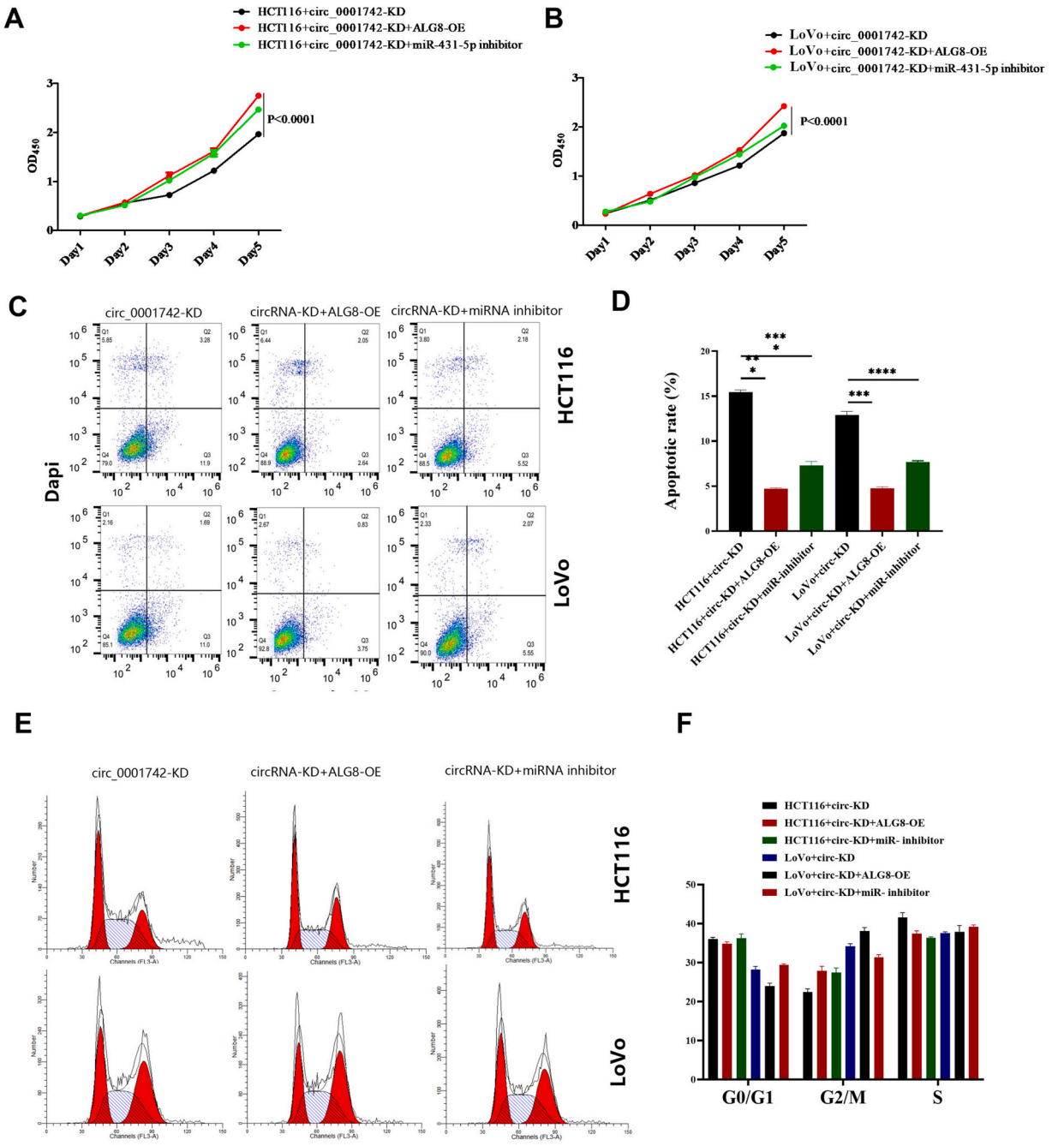

Fig. 5. Hsa_circ_0001742 modulates the expression of ALG8, an endogenous target of hsa_miR_431-5p. (A, B) CCK-8 assays were performed after cells were cotransfected with different vectors. Compared with control cells, the expression level of ALG8 was increased in LoVo and HCT116-circ_0001742-KD cells, and the proliferation ability of cells was significantly increased. The level of miR-431-5p was decreased in circ_0001742-KD cells, and the proliferation ability of the cells was significantly increased. (C, D) The results of flow-through apoptosis experiments showed that, compared with control cells, the expression level of ALG8 was increased in HCT116 and LoVo circ_0001742-KD cells, and the apoptosis level of cells was significantly decreased. The level of miR-431-5p was decreased in circ_0001742-KD cells, and the apoptosis level of the cells was significantly decreased. (E, F) The results of flow cytometry cycle experiments showed that compared with control cells, the number of cells in the G0 phase was significantly decreased in HCT116 and LoVo circ_0001742-KD cells with increased ALG8 expression levels, and the number of cells in the G2 phase was significantly increased. The decreased level of miR-431-5p in circ_0001742-KD cells had no significant effect in the G0 phase, significantly decreased in the G2 phase, and significantly increased in the S phase. *P < 0.05, **P < 0.01, ***P < 0.001.

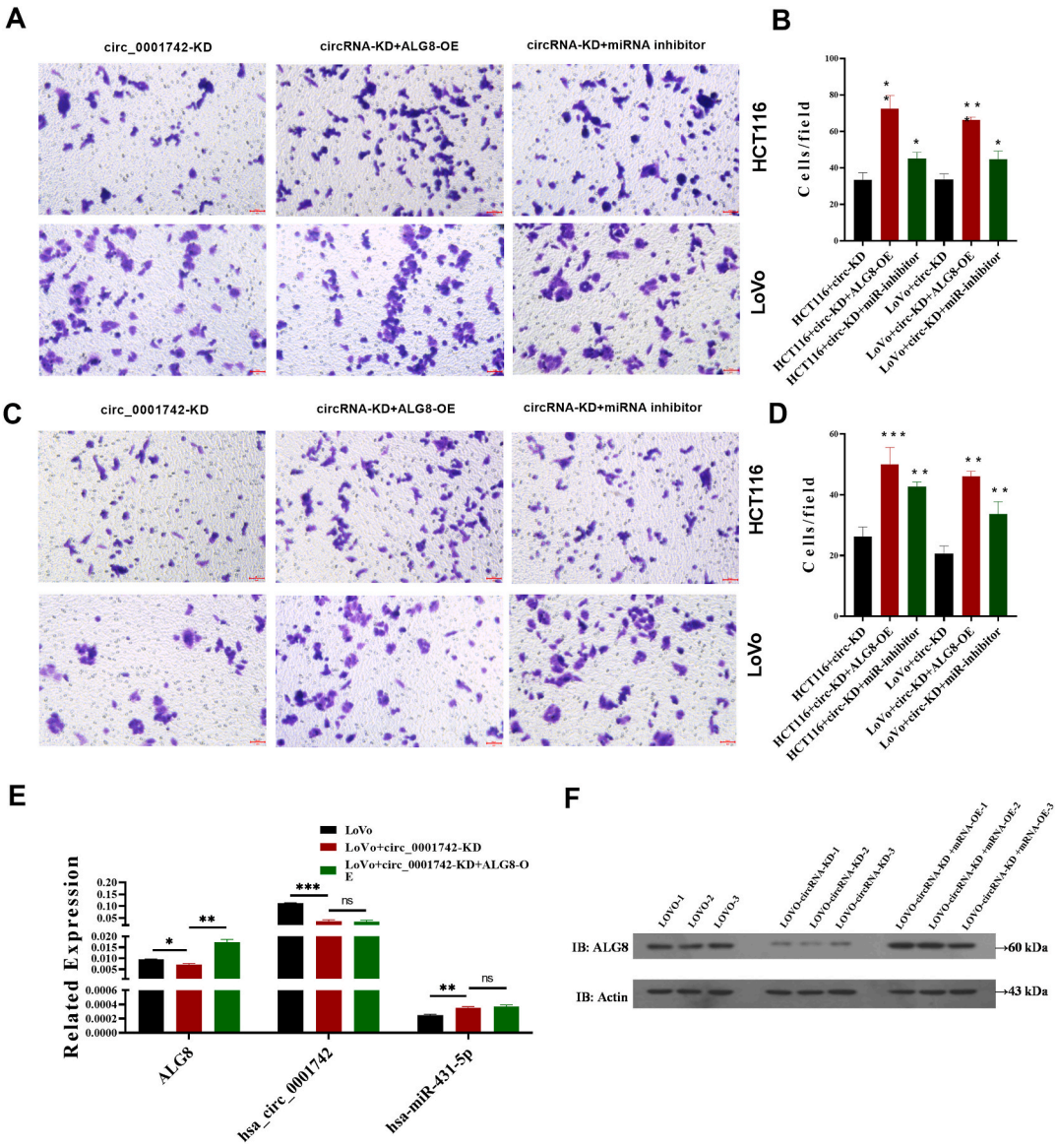

Fig. 6. Hsa_circ_0001742 modulates the expression of ALG8, an endogenous target of hsa_miR_431-5p. (A,B) The results of Transwell experiments showed that compared with control cells, the expression level of ALG8 was increased in HCT116 and LoVo circ_0001742-KD cells, and the cell migration ability was significantly increased. The level of miR-431-5p was decreased in circ_0001742-KD cells, and the migration ability of the cells was significantly increased. (C,D) The results of the Matrigel-Transwell experiment showed that compared with the control cells, the expression level of ALG8 was increased in HCT116 and LoVo circ_0001742-KD cells, and the invasive ability of the cells was significantly increased. The level of miR-431-5p was decreased in circ_0001742-KD cells, and the invasive ability of the cells was significantly increased. (E) The results of RT-qPCR experiments showed that compared with the inoculated control cells, ALG8 was significantly decreased in the tumor tissue formed after knockdown of hsa_circ_0001742 in the cells, and the expression level of ALG8 in the cells was significantly increased after ALG8 replenishment. Compared with inoculated control cells, ALG8 was significantly decreased in tumor tissues formed after knockdown of hsa_circ_0001742 in cells, and the expression level of ALG8 in cells was significantly increased after ALG8 replenishment. (F) The relative ALG8 protein expression levels in tumor tissues were analyzed by western blotting. *P < 0.05, **P < 0.01, ***P < 0.001 *P < 0.05, **P < 0.01, ***P < 0.001.

3.7. The circ_0001742/miR-431-5p/ALG8 axis and CRC progression

We found that circ_0001742-silenced tumors were much smaller in size and weighed less than their LoVo cell counterparts (Fig. 8A). In addition, the circ_0001742-silenced and ALG8-overexpressing groups had larger sizes and higher weights than the LoVo control cells (Fig. 8B–C). Likewise, the results of immunohistochemistry and haematoxylin-eosin staining revealed that the circ_0001742 silencing group had lower expression of ALG8 than the control group. Otherwise, the circ_0001742-silenced and ALG8-overexpressing groups had higher expression of ALG8 than the LoVo control cell group (Fig. 8D). These results demonstrated that the

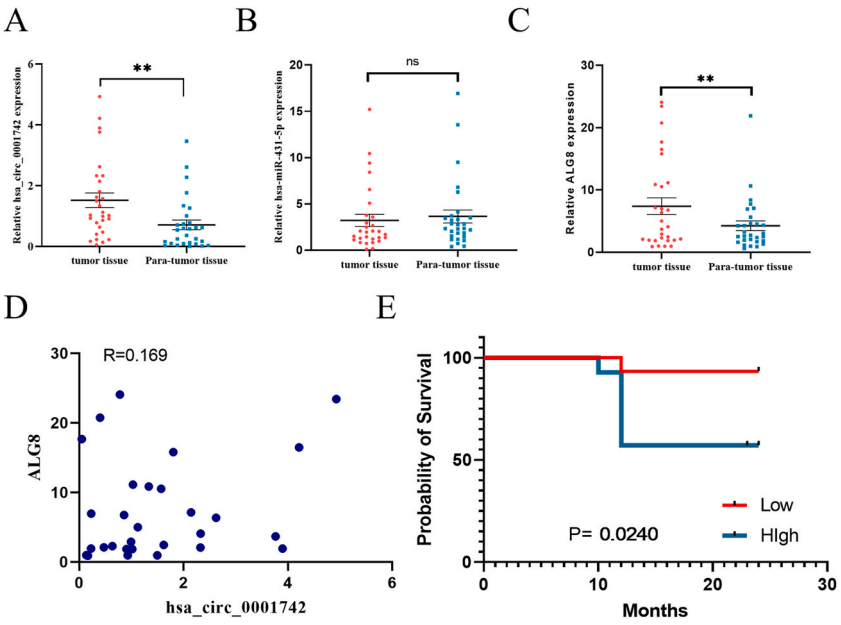

Fig. 7. Expression of hsa_circ_0001742, hsa_miR_431-5p and ALG8 in relation to prognosis. (A–C) RT-qPCR to detect the expression levels of hsa_circ_0001742 (A), hsa_miR_431-5p (B) and ALG8 (C) in 29 pairs of clinical samples; (D) correlation between hsa_circ_0001742 and ALG8 expressions in clinical samples; (E) database analysis of hsa_circ_ 0001742 expression in relation to the prognosis of colorectal cancer patients. *P < 0.05, **P < 0.01, ***P < 0.001.

circ_0001742/miR-431-5p/ALG8 axis has a great effect on the progression of CRC.

4. Discussion

A high level of metastasis causes a dismal prognosis and the vast majority of cancer-related deaths for CRC patients [31]. Despite the diagnostic advances that have been made, even the 5-year survival rate for stage IV patients with CRC who receive treatment is merely 10 % [32]. When the traditional treatment schemes meet a bottleneck, many scholars and clinicians turn their research direction to the analysis of targeted therapies. As a class of abundant noncoding RNA molecules across all eukaryotes, circRNAs present stronger stability than linear RNAs [33]. Importantly, emerging studies have demonstrated that circRNAs could be potential diagnostic or predictive biomarkers in cancer [34,35]. However, the key deregulated circRNAs and their mechanisms in CRC are vague.

In the present study, we screened the potential driver circRNAs responsible for metastasis initiation in CRC pathogenesis and identified circRNA expression profiles in CRC cells with different metastatic abilities by RNA sequencing. We demonstrated that circ_0001742 was greatly upregulated in metastasis-initiating subgroups of CRC cells. At the tissue level, we demonstrated that circ_0001742 was more abundant in CRC tissues than in adjacent normal tissues. In addition, we found that increased circ_0001742 expression tended to be linked with unfavourable prognosis in CRC patients.

At the cell line level, we revealed that circ_0001742 was more highly expressed in high metastatic potential cells than in low metastatic potential cells. More importantly, we found that overexpression of circ_0001742 in cell lines can improve cell activity and promote migration. Bioinformatics predictions and the luciferase reporter showed that circ_0001742 could target miR-431-5p. Mechanistically, circ_0001742 acted as a sponge of miR-431-5p, and miR-431-5p could target the 3′UTR of ALG8. More interestingly, the xenograft tumour model demonstrated that the circ_0001742/miR-431-5p/ALG8 axis influences the progression of CRC in vivo. The results of this study show that circ_0001742 affects the development of colorectal cancer.

Current studies have shown that most circRNAs are abundant and stable in the cytoplasm and regulate the circRNA-miRNA–mRNA axis [36,37]. Our study also identified that circ_0001742 is mainly distributed in the cytoplasm and acts as a miRNA sponge. Its potential regulatory functions in CRC cells rely on interacting with miR-431-5p processing. In addition, overexpression of circ_0001742 mediated the adverse progression of CRC cells. MiR-431-5p has been demonstrated to be a tumour suppressor miRNA in multiple types of cancer. It can induce cell apoptosis and inhibit cell proliferation and migration by targeting oncogenes in hepatocellular carcinoma, osteosarcoma and lung cancer [38–40]. To identify downstream genes regulated by miR-431-5p in CRC cells, this study used bioinformatics analysis to predict potential target genes. The bioinformatics analysis revealed ALG8 as one of the targets of miR-431-5p, and qPCR validated this postulation.

Previous studies reported that, as an oestrogen receptor (ER) membrane protein, ALG8 encodes a-1,3-glucosyltransferase and plays an essential role in attaching the second glucose residue to a lipid-linked oligosaccharide for N-linked glycosylation before it is transferred to the nascent peptide [41]. Moreover, we found that overexpression of circ_0001742 notably increased ALG8 expression. The expression of ALG8 was significantly downregulated in circ_0001742-knockdown cells. In addition, the results of the xenograft

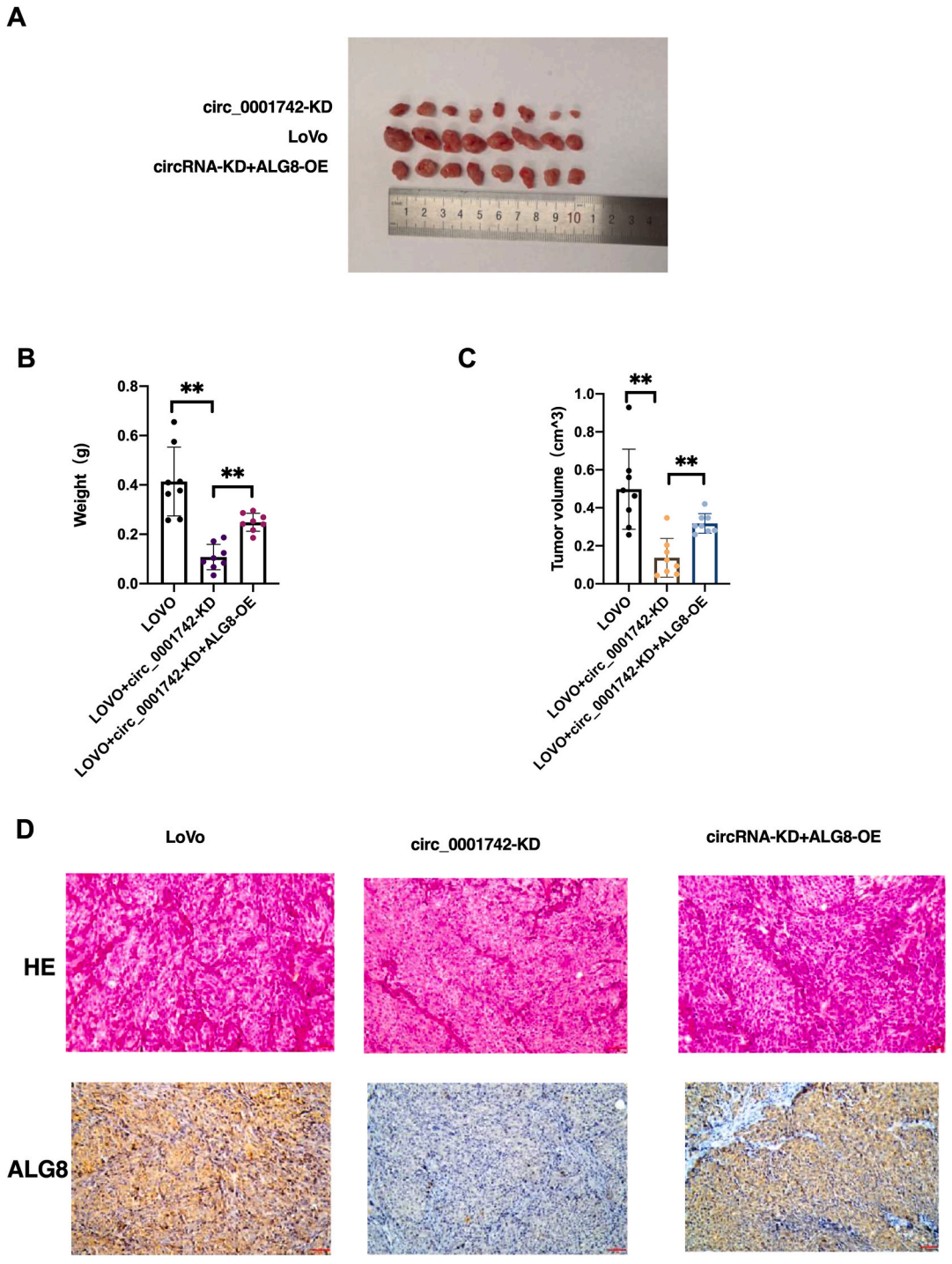

Fig. 8. Hsa_circ_0001742 promotes CRC progression in vivo. (A) Image of subcutaneous xenograft tumors. Nude mice were injected with 5 × 106 LoVo cells (N = 8 for each group). Tumors were extracted after 30 days. (B) Tumor weight in each group at the end of the experiment. (C) Analysis of tumor volume of mice. (D) Haematoxylin-eosin staining and histological analysis of tumor tissues by haematoxylin and eosin staining. Immunohistochemistry of ALG8 in subcutaneous tumors. Scale bar, 100 μm.

tumour model showed that the circ_0001742-silenced and ALG8-overexpressing groups had larger sizes and higher weights than the control group. Likewise, the Western blotting results showed a similar tendency. Therefore, the circ_0001742/miR-431-5p/ALG8 axis can promote the adverse progression of CRC.

Although this study has made the above progress, there are still some shortcomings. First, although we found differential expression

of circ_0001742 in CRC cells with different metastatic potential, future validation in larger plasma and cancer tissues is needed. Second, studies have identified several RNA-binding proteins (RBPs) that interact with miRNA processing machinery, and it would be interesting to further investigate the effect of RBPs involved in the circ_0001742-related mechanism.

5. Conclusion

Circ_0001742 was positively associated with adverse progression of cancer cells in vivo and in vitro. In particular, circ_0001742 promoted the progression of colorectal cancer, such as promoting cell proliferation, inhibiting apoptosis, and promoting invasion and migration of colorectal cancer. through the circ_0001742/miR-431-5p/ALG8 axis, suggesting that circ_0001742 could be a promising anti-metastasis therapeutic target for CRC.

Availability of data and materials

All data obtained or analyzed in the present study are included in the manuscript and its Supplementary Information. The datasets used and/or analyzed during the current study are available from the corresponding authors (tangweizhong@gxmu.edu.cn) on reasonable request.

Funding information

This work was supported by the Guangxi Natural Science Foundation Program (2022GXNSFAA035505)

Ethics statement

The study was conducted in accordance with the principles of the Declaration of Helsinki principles. The studies involving human participants were reviewed and approved by First Affiliated Hospital and Affiliated Tumor Hospital of Guangxi Medical University Ethics Committee. Informed Consent: All study participants signed informed consents.(No. LW2023013.)Animal Studies: Mice were maintained in accordance with the Guidelines of the Institutional Animal Careand Use Committee of Guangxi Medical University. The Medical Ethics Committee of Guangxi Medical University Cancer Hospital has approved the protocol.

CRediT authorship contribution statement

Jiahao Huang: Writing – review & editing, Writing – original draft, Visualization, Validation, Data curation, Conceptualization. **Fengyun Cong:** Writing – original draft, Visualization, Software, Conceptualization. **Yang Zhao:** Writing – original draft, Methodology, Investigation, Formal analysis. **Jinglian Chen:** Resources, Data curation, Conceptualization. **Tao Luo:** Writing – review & editing, Resources, Methodology. **Weizhong Tang:** Writing – review & editing, Writing – original draft, Data curation, Conceptualization.

Declaration of competing interest

The authors declare that they have no known competing financial interests or personal relationships that could have appeared to influence the work reported in this paper.

Acknowledgments

This work was supported by the Guangxi Cancer Hospital Biological Resource Bank for providing the samples.

Appendix A. Supplementary data

Supplementary data to this article can be found online at https://doi.org/10.1016/j.heliyon.2024.e34660.

References

[1] Hyuna Sung, Jacques Ferlay, Rebecca L. Siegel, Mathieu Laversanne, Isabelle Soerjomataram, Ahmedin Jemal, Freddie Bray, Global cancer statistics 2020: GLOBOCAN estimates of incidence and mortality worldwide for 36 cancers in 185 countries, CA A Cancer J. Clin. 71 (3) (2021) 209–249.
[2] Ernest T. Hawk, Bernard Levin, Colorectal cancer prevention, J. Clin. Oncol. 23 (2) (2005) 378–391.
[3] Amanda M. Pattison, Dante J. Merlino, Erik S. Blomain, Scott A. Waldman, Guanylyl cyclase C signaling axis and colon cancer prevention, World J. Gastroenterol. 22 (36) (2016) 8070.
[4] Chu Qiao, Haiying Wang, Qiutong Guan, Minjie Wei, Zhenhua Li, Ferroptosis-based nano delivery systems targeted therapy for colorectal cancer: insights and future perspectives, Asian J. Pharm. Sci. 17 (5) (2022) 613–629.

[5] Jing Zhang, Qizhi Luo, Xin Li, Junshuang Guo, Quan Zhu, Xiaofang Lu, Leiyan Wei, et al., Novel role of immune-related non-coding RNAs as potential biomarkers regulating tumour immunoresponse via MICA/NKG2D pathway, Biomark. Res. 11 (1) (2023) 86.
[6] Jing Sun, Lu Wu, Meng Wu, Qizhan Liu, Hong Cao, Non-coding RNA therapeutics: towards a new candidate for arsenic-induced liver disease, Chem. Biol. Interact. (2023) 110626.
[7] William R. Jeck, E. Sharpless Norman, Detecting and characterizing circular RNAs, Nat. Biotechnol. 32 (5) (2014) 453–461.
[8] Lasse S. Kristensen, B. Hansen Thomas, Morten T. Venø, Jørgen Kjems, Circular RNAs in cancer: opportunities and challenges in the field, Oncogene 37 (5) (2018) 555–565.
[9] Hongwei Su, Tao Tao, Zhao Yang, Xing Kang, Xu Zhang, Danyue Kang, Song Wu, Chong Li, Circular RNA cTFRC acts as the sponge of MicroRNA-107 to promote bladder carcinoma progression, Mol. Cancer 18 (2019) 1–15.
[10] Xu Guo, Congying Gao, Dong-Hua Yang, Shenglong Li, Exosomal circular RNAs: a chief culprit in cancer chemotherapy resistance, Drug Resist. Updates 67 (2023) 100937.
[11] Di Leva, Gianpiero, Michela Garofalo, Carlo M. Croce, MicroRNAs in cancer, Annu. Rev. Pathol. 9 (2014) 287–314.
[12] Thomas B. Hansen, Trine I. Jensen, Bettina H. Clausen, Jesper B. Bramsen, Bente Finsen, Christian K. Damgaard, Kjems Jørgen, Natural RNA circles function as efficient microRNA sponges, Nature 495 (7441) (2013) 384–388.
[13] Wenhao Weng, Qing Wei, Shusuke Toden, Kazuhiro Yoshida, Takeshi Nagasaka, Toshiyoshi Fujiwara, Sanjun Cai, Huanlong Qin, Yanlei Ma, Ajay Goel, Circular RNA ciRS-7—a promising prognostic biomarker and a potential therapeutic target in colorectal cancer, Clin. Cancer Res. 23 (14) (2017) 3918–3928.
[14] Zhuoan Cheng, Chengtao Yu, Shaohua Cui, Hui Wang, Haojie Jin, Cun Wang, Botai Li, et al., c irctp63 functions as a cerna to promote lung squamous cell carcinoma progression by upregulating foxm1, Nat. Commun. 10 (1) (2019) 3200.
[15] Yang Li, Yu-zheng Ge, Luwei Xu, Ruipeng Jia, Circular RNA ITCH: a novel tumor suppressor in multiple cancers, Life Sci. 254 (2020) 117176.
[16] Yuejiao Wang, Kailin Zhang, Xiaowei Yuan, Neili Xu, Shuai Zhao, Linxin Hou, Lili Yang, Ning Zhang, miR-431-5p regulates cell proliferation and apoptosis in fibroblast-like synoviocytes in rheumatoid arthritis by targeting XIAP, Arthritis Res. Ther. 22 (2020) 1–10.
[17] Wei Huang, Chong Zeng, Shanbiao Hu, Lei Wang, Jie Liu, ATG3, a target of miR-431-5p, promotes proliferation and invasion of colon cancer via promoting autophagy, Cancer Manag. Res. (2019) 10275–10285.
[18] Emilie Cornec-Le Gall, Vicente E. Torres, Peter C. Harris, Genetic complexity of autosomal dominant polycystic kidney and liver diseases, J. Am. Soc. Nephrol. 29 (1) (2018) 13–23.
[19] Patria Di, Laura Giosuè Annibalini, Amelia Morrone, Lorenzo Ferri, Roberta Saltarelli, Luca Galluzzi, Aurora Diotallevi, et al., Defective IGF-1 prohormone N-glycosylation and reduced IGF-1 receptor signaling activation in congenital disorders of glycosylation, Cell. Mol. Life Sci. 79 (3) (2022) 150.
[20] Xianqiu Wu, Bin Wang, Yaorong Su, Dongtian He, Haixin Mo, Mingzhu Zheng, Zijie Meng, et al., ALG8 fuels stemness through glycosylation of the WNT/Beta-Catenin signaling pathway in colon cancer, DNA Cell Biol. 41 (12) (2022) 1075–1083.
[21] Ziting Zhang, You Ji, Nan Hu, Qinqi Yu, Xinrui Zhang, Jie Li, Fenglei Wu, Huae Xu, Qiyun Tang, Xiaolin Li, Ferroptosis-induced anticancer effect of resveratrol with a biomimetic nano-delivery system in colorectal cancer treatment, Asian J. Pharm. Sci. 17 (5) (2022) 751–766.
[22] Sebastian Memczak, Marvin Jens, Antigoni Elefsinioti, Francesca Torti, Janna Krueger, Agnieszka Rybak, Luisa Maier, et al., Circular RNAs are a large class of animal RNAs with regulatory potency, Nature 495 (7441) (2013) 333–338.
[23] Yuan Gao, Jingyang Zhang, Fangqing Zhao, Circular RNA identification based on multiple seed matching, Briefings Bioinf. 19 (5) (2018) 803–810.
[24] Liang Zhou, Jiahao Chen, Zhizhong Li, Xianxin Li, Xueda Hu, Yi Huang, Xiaokun Zhao, et al., Integrated profiling of microRNAs and mRNAs: microRNAs located on Xq27. 3 associate with clear cell renal cell carcinoma, PLoS One 5 (12) (2010) e15224.
[25] Liang-Yan Chen, Zhi Zheng, Lian Wang, Yuan-Yuan Zhao, Min Deng, Yu-Hong Liu, Yan Qin, et al., NSD2 circular RNA promotes metastasis of colorectal cancer by targeting miR-199b-5p-mediated DDR1 and JAG1 signalling, J. Pathol. 248 (1) (2019) 103–115.
[26] Huijuan Zhang, Yaping Wang, Mengting Li, Kexuan Cao, Zijun Qi, Ling Zhu, Zhenzhong Zhang, Lin Hou, A self-guidance biological hybrid drug delivery system driven by anaerobes to inhibit the proliferation and metastasis of colon cancer, Asian J. Pharm. Sci. 17 (6) (2022) 892–907.
[27] Hongbo Zou, Shuang Wang, Songtao Wang, Hong Wu, Jing Yu, Qian Chen, Wei Cui, et al., SOX5 interacts with YAP1 to drive malignant potential of non-small cell lung cancer cells, Am. J. Cancer Res. 8 (5) (2018) 866.
[28] Weibing Zhou, Xiaoyan Liao, Juan Huang, p12 CDK2-AP1 inhibits breast cancer cell proliferation and in vivo tumor growth, J. Cancer Res. Clin. Oncol. 138 (2012) 2085–2093.
[29] Kai Han, Feng-Wei Wang, Chen-Hui Cao, Ling Han, Jie-Wei Chen, Ri-Xin Chen, Zi-Hao Feng, et al., CircLONP2 enhances colorectal carcinoma invasion and metastasis through modulating the maturation and exosomal dissemination of microRNA-17, Mol. Cancer 19 (2020) 1–18.
[30] Petar Glažar, Panagiotis Papavasileiou, Nikolaus Rajewsky, circBase: a database for circular RNAs, RNA 20 (11) (2014) 1666–1670.
[31] Rebecca L. Siegel, Kimberly D. Miller, Ann Goding Sauer, Stacey A. Fedewa, Lynn F. Butterly, Joseph C. Anderson, Andrea Cercek, Robert A. Smith, Ahmedin Jemal, Colorectal cancer statistics, 2020, CA A Cancer J. Clin. 70 (3) (2020) 145–164.
[32] Evelien Dekker, Pieter J. Tanis, Jasper LA. Vleugels, Pashtoon M. Kasi, Michael B. Wallace, Colorectal cancer, Lancet 394 (10207) (2019) 1467–1480.
[33] Ri-Xin Chen, Xin Chen, Liang-Ping Xia, Jia-Xing Zhang, Zhi-Zhong Pan, Xiao-Dan Ma, Kai Han, et al., N 6-methyladenosine modification of circNSUN2 facilitates cytoplasmic export and stabilizes HMGA2 to promote colorectal liver metastasis, Nat. Commun. 10 (1) (2019) 4695.
[34] Julia Salzman, Raymond E. Chen, Mari N. Olsen, Peter L. Wang, Patrick O. Brown, Cell-type specific features of circular RNA expression, PLoS Genet. 9 (9) (2013) e1003777.
[35] Ling-Ling Chen, The biogenesis and emerging roles of circular RNAs, Nat. Rev. Mol. Cell Biol. 17 (4) (2016) 205–211.
[36] William R. Jeck, Jessica A. Sorrentino, Kai Wang, Michael K. Slevin, Christin E. Burd, Jinze Liu, William F. Marzluff, Norman E. Sharpless, Circular RNAs are abundant, conserved, and associated with ALU repeats, RNA 19 (2) (2013) 141–157.
[37] Julia Salzman, Charles Gawad, Peter Lincoln Wang, Norman Lacayo, Patrick O. Brown, Circular RNAs are the predominant transcript isoform from hundreds of human genes in diverse cell types, PLoS One 7 (2) (2012) e30733.
[38] Qian Jiang, Li Cheng, Daiyuan Ma, Yanli Zhao, FBXL19-AS1 exerts oncogenic function by sponging miR-431-5p to regulate RAF1 expression in lung cancer, Biosci. Rep. 39 (1) (2019) BSR20181804.
[39] Shengliang Sun, Lei Fu, Gen Wang, Jianli Wang, Liping Xu, MicroRNA-431-5p inhibits the tumorigenesis of osteosarcoma through targeting PANX3, Cancer Manag. Res. (2020) 8159–8169.
[40] Qinglei Kong, Jianhua Han, Hong Deng, Feilong Wu, Shaozhong Guo, Zhiqiang Ye, miR-431-5p alters the epithelial-to-mesenchymal transition markers by targeting UROC28 in hepatoma cells, OncoTargets Ther. (2018) 6489–6503.
[41] Jörg Breitling, Markus Aebi, N-linked protein glycosylation in the endoplasmic reticulum, Cold Spring Harbor Perspect. Biol. 5 (8) (2013) a013359.